Dick, JJ, Tetzlaff, D, Bradford, J and Soulsby, C

Using repeat electrical resistivity surveys to assess heterogeneity in soil moisture dynamics under contrasting vegetation types

Article

Using repeat electrical resistivity surveys to assess heterogeneity in soil moisture dynamics under contrasting vegetation types

Jonathan Dick[1, 5], Doerthe Tetzlaff[1,2,3], John Bradford[4], Chris Soulsby[1]

[1]Northern Rivers Institute, University of Aberdeen, Aberdeen, UK (j.j.dick@ljmu.ac.uk)

[2] IGB Leibniz Institute of Freshwater Ecology and Inland Fisheries
[3] Humboldt University Berlin
[4]Colarado School of Mines
[5]Liverpool John Moores University

Abstract

As the relationship between vegetation and soil moisture is complex and reciprocal, there is a need to understand how spatial patterns in soil moisture influence the distribution of vegetation, and how the structure of vegetation canopies and root networks regulates the partitioning of precipitation. Spatial patterns of soil moisture are often difficult to visualise as usually, soil moisture is measured at point scales, and often difficult to extrapolate. Here, we address the difficulties in collecting large amounts of spatial soil moisture data through a study combining plot- and transect-scale electrical resistivity tomography (ERT) surveys to estimate soil moisture in a 3.2 km^2 upland catchment in the Scottish Highlands. The aim was to assess the spatio-temporal variability in soil moisture under Scots pine forest (*Pinus sylvestris*) and heather moorland shrubs (*Calluna* vulgaris); the two dominant vegetation types in the Scottish Highlands. The study focussed on one year of fortnightly ERT surveys. The surveyed resistivity data was inverted and Archie's law was used to calculate volumetric soil moisture by estimating parameters and comparing against field measured data. Results showed that spatial soil moisture patterns were more heterogeneous in the forest site, as were patterns of wetting and drying, which can be linked to vegetation distribution and canopy structure. The heather site showed a less heterogeneous response to wetting and drying, reflecting the more uniform vegetation cover of the shrubs. Comparing soil moisture temporal variability during growing and non-growing seasons revealed further contrasts: under the heather there was little change in soil moisture during the growing season. Greatest changes in the forest were in areas where the trees were concentrated reflecting water uptake and canopy partitioning. Such differences have implications for climate and land use changes; increased forest cover can lead to greater spatial variability, greater growing season temporal variability, and reduced levels of soil moisture, whilst projected decreasing summer precipitation may alter the feedbacks between soil moisture and vegetation water use and increase growing season soil moisture deficits.

Keywords: Electrical resistivity tomography; soil moisture; forest; moorland

1. Introduction

Soil moisture is a fundamental, highly dynamic, characteristic of terrestrial ecosystems, which regulates vegetation productivity (Rodríguez-Iturbe and Porporato, 2007) and strongly influences biogeochemical processes (Robinson et al., 2008). The relationship between vegetation cover and soil moisture is complex (Entekhabi et al., 1996; Zribi et al., 2010). Soil moisture as the primary source of water to plants commonly affects vegetation distribution (Stephenson 1990; Rodriguez-Iturbe et al., 1999). In turn, the structure of vegetation canopies regulates water partitioning into interception losses, and net precipitation as through-fall and stem flow (Helvey and Patric, 1965; Ford and Deans, 1978; Pypker et al., 2005). Spatial differences in inputs, together with complex patterns of water uptake from highly distributed root networks, often create marked heterogeneity in soil moisture distribution and associated dynamics (Liang et al., 2011; Coenders-Gerrits et al., 2013).

A changing climate is likely to alter the spatial and temporal dynamics of soil moisture in many areas and this may, in turn, affect plant distribution and growth (Rodriguez-Iturbe et al., 1999; Seneviratne et al., 2010). Climate change projections in many northern maritime regions infer a shift in precipitation distributions towards increased winter inputs but reduced growing season rainfall (Murphy et al., 2009). With projected increased temperatures, this could result in potential water stresses during growing seasons in many regions (Reyer et al., 2013), which may lead to shifting vegetation patterns (Porporato et al., 2004; Rigling et al., 2013). With differences in water partitioning between vegetation types, it is important to understand how potential climatic and vegetation changes will affect the soil moisture in the landscape.

Measuring soil moisture at the point scale is relatively easy, however, marked heterogeneity in the subsurface (Cosh et al., 2004) dictates that it is difficult to upscale to landscape-scale processes (i.e. point to plot or hillslope or catchment scale) (Vereecken et al., 2008; Brocca et al., 2012; Tetzlaff et al., 2014). Heterogeneity in the subsurface also leads to spatial differences in soil moisture, something which may not be easily visualised using point measurements. Whilst there has been some success in using multiple point measurements to study the effects of vegetation on soil moisture (e.g. Teuling et al., 2006) there remains a need to assess processes occurring at larger scales and link these to vegetation-water interactions more clearly. New technologies such as cosmic ray sensors have potential in working passively over large areas to collect real-time data (Zreda et al., 2008), and have been successfully used to image field scale root zone soil moisture (Peterson et al., 2016). Unfortunately, their use is limited when considering small scale soil moisture patterns, as their spatial resolution is low (Zreda et al., 2008) Over the past few decades, geophysical techniques such as electrical resistivity tomography (ERT) have proven to be useful in estimating the soil moisture content of the vadose zone. Successful studies have used 2D transects (e.g. Schwartz et al., 2008; Brunet et al., 2010; Ain-Lhout et al., 2016) and 3D plots (e.g. al Hagrey, 2007; Srayeddin et al., 2009; Garré et al., 2011; Beff et al., 2013; Boaga et al., 2013; Chambers et al., 2014) to gain insight into soil moisture distributions.

ERT has great potential for understanding soil moisture variations at the plot and hillslope scale, and the way in which this variability is affected by vegetation (Zhou et al., 2001). Archie's law (Archie 1942) is commonly used to estimate soil moisture from electrical resistivity measurements (e.g. Zhou et al, 2001; Brunet et al, 2010; Schwartz et al, 2008). Specifically, Archie's law relates the electrical conductivity of a granular rock to its porosity, saturation and fluid conductivity. Difficulties in the use of Archie's law arise from the requirement to measure and estimate these variables and parameters, something essential when using ERT to estimate soil moisture. These parameters can be obtained from measurements conducted in the field (Zhou et al., 2001), lab (Brunet et al., 2010), or both (Schwartz et al. 2008).

Here, we use ERT to estimate soil moisture dynamics in a catchment in the Scottish Highlands, which is broadly representative of northern, formerly glaciated landscapes (Soulsby et al., 2015). Two soil-vegetation units dominate the catchment, namely shrub and forest vegetation on freely draining podzolic soils. Previous empirical and modelling studies have used hydrometric and tracer data to infer significant groundwater stores in drift aquifers (e.g. Soulsby et al., 2007; Birkel et al., 2010; Tetzlaff et al., 2014). Soulsby et al. (2016) previously used spatially distributed ERT surveys to characterise the distribution, thickness and properties (including water content) of extended glacial drifts in the study catchment. Here, we build on this work and seek to test the hypothesis that the influence of vegetation on spatial volumetric soil moisture patterns and dynamics will be different under heather and forest vegetation types due to the canopy structure and distribution of vegetation.

Our specific objectives were to:

(a) Estimate plot scale soil moisture from repeat plot- and transect-scale ERT measurements using the generalised Archie's law and time-domain reflectometry (TDR) soil moisture measurements

(b) Assess the spatial and temporal soil moisture heterogeneity within the rooting zone of the forest and heather sites to investigate the differences between vegetation types.

2. Study site

The study catchment, the Bruntland Burn (3.2 km^2) in NE Scotland, is described elsewhere in detail (Tetzlaff et al., 2014; Dick et al., 2014). Elevations range from 248 to 539 m.a.s.l, with mean slopes of 13°. The bedrock geology is predominantly granitic, bordered by schist and other metamorphic rocks in the south/southeast. The area was glaciated during the last glacial maximum, and as a result has a subdued topography with a wide flat valley bottom. The landscape is drift-draped, with shallow drift on the upper hillslopes grading to deeper glacial fills in the valley bottom (up to 40 m deep - Soulsby et al, 2016). The soils in the catchment are typical of these environments, with freely draining rankers and podzolic soils on the hillslopes, and more hydrologically responsive gleys (on the lower hillslopes) and deep peats (Histosols), up to 4 m deep, in the flat valley bottoms.

The vegetation is representative of many UK upland catchments. It is heavily influenced by historic land management practices with a long history of forest clearance, overgrazing by deer (*Cervus elaphus*) and sheep (*Ovis aries*), and moorland burning for grouse (*Lagopus lagopus*). As such, vegetation is dominated by heather shrubs (e.g. *Calluna vulgaris, Erica tetralix*) and grass (*Molinia caerulea*) moorland vegetation on the freely draining podzolic hillslopes and rankers. Due to the aforementioned land management practices, forest coverage is typically low, with mainly Scots Pine (*Pinus sylvestris*) on freely draining podzolic soils (Fig 1). Forests are focussed on areas where deer are excluded.

Two experimental locations were chosen in characteristic areas and both are representative of the dominant soil-vegetation units in the catchment (Fig 1). Both locations were in close proximity to long-term soil moisture measurement sites. One site was chosen under forest vegetation and one in the heather moorland, both on podzolic soils. The heather site was located on the southwest side near the catchment outlet, and was situated on a topographically flat location (with some small micro-topography at the cm scale). The heather is around 0.2-0.3 m tall with 95% of roots in the upper 0.2 m of the soil profile (Sprenger et al.,, 2017), with a fairly dense and low canopy. In the heather, 21% of the precipitation is lost to interception. Transpiration in the heather site is estimated as 97 mm during the growing season (Wang et al., 2017). At the forest site, 95% of Scots Pine roots are contained within the upper 0.48 m of the soil profile (Haria and Price, 2000), and average canopy cover is 68%, varying between 20% and 90%, (Soulsby et al., 2017) (Fig 2). Around 45% of the gross precipitation is lost to interception (Wang et al., 2017). Transpiration estimates suggest 111 mm of transpired water during the growing season (derived from sap flow measurements between mid-April-early September; Wang et al., 2017).

3. Data and Methods

3.1 Hydrometric data

Meteorological data is required for temperature correction of electrical resistivity to a standard temperature, for which data primarily came from two sources, with hourly soil and air temperature data (to temperature-correct the resistivity data) from the MetOffice Aboyne No.2 station 20km away, through the British Atmospheric Data Centre (BADC). Soil temperature was averaged over the first 0.5 m of the soil profile. This data was supplemented with air temperature data from an automatic weather station situated in the Bruntland Burn, where precipitation and net radiation were measured every 15 minutes. The data from the AWS was then used to calculate PET using the method of Dunn and Mackay (1995).

Each of the study locations was instrumented for VSM measurements consisting of one soil moisture station per location. Each station was equipped for measuring VSM at 15 minutes intervals using

Campbell Scientific CS616 probes (c.f. Mittelbach et al., 2012) connected to a CR800X data logger. The same installation setup was used at each location and was described in detail by Geris et al. (2015). Probes were installed horizontally at 3 depths (0.15, 0.2 and 0.5 m) corresponding to the O, E, and B soil horizons, with two probes at each depth, with the VSM from both averaged. This was carried out to provide a replicate and account for subsurface heterogeneity, something which can lead to variable TDR VSM measurements. While CS616 probes are useful in collecting high temporal resolution datasets, there are potential problems associated with installation in stone rich soils, with measurements rods needing to remain the same distance apart and in contact with the surrounding soil. This can lead to problems when attempting to install spatially dense arrays for soil moisture measurement.

3.2 Electrical resistivity tomography

We collected ERT data using an IRIS instruments SysCal Pro 72 electrode system. An electrical current was injected through two of the electrodes (the source), and the potential difference was then measured between two other electrodes (Zonge et al., 2005; Binley et al., 2015). This was then repeated automatically, with different separations between the electrodes, depending on array and measurement length. We considered that when the electrodes are further apart, a greater proportion of the current flows deeper into the earth and, consequently, is influenced by deeper structures in the subsurface, and not just the surface.

At the forest site, one 7 by 8 m plot, and one 8.75 m transect were installed. At the heather site, one 3.5 by 4 m plot and one 8.75 m transect was installed. The forest plot was situated north of the catchment outlet, and was the topographically more variable site (surface elevation range: 0.9 m) (Fig 1). For all surveys, a dipole-dipole array was used, as this is more sensitive to lateral changes (Zonge et al., 2005), which is of interest when investigating spatial changes in soil moisture. While the better signal to noise ratio of Wenner and Wenner-Schlumberger arrays would have been desirable, the inability to run these over multiple channels, and increased survey time made it impractical.

For the plot surveys, we placed 72 electrodes in a 8x9 node rectangular grid to visualise plot scale spatial VSM down to 0.5 m depths. A 3D orthogonal array was used, and was created using the Electre Pro software from Iris Instruments. All plot surveys used 6 stacks and 800 maximum voltage and a transmit time of 1000 ms. A 1 m grid spacing was used in the forest location, and a 0.5 m grid spacing in the heather location, giving mesh sizes of 0.5 m and 0.25 m respectively. The different spacing between the two plots was used to increase the resolution in the heather site because of the smaller size of the vegetation and the shallower root zone at that site. It must be noted that the difference in electrode spacing between surveys changes the resolution of the survey, as the resolution of an array is closely linked to the distance between the receiving and transmitting electrodes, with smaller distances increasing the resolution. This was deemed to be a reasonable trade-off as it increased the useful information gained with the higher resolution. The electrodes were 0.05 m x 0.05 m rectangular stainless-steel mesh (Tomaškovičová et al., 2016), and placed permanently by burying 0.05 m below the surface (Fig 1). These electrodes were chosen as the rocky subsurface made achieving a good contact difficult when using standard metal pegs. All plot data were collected for 6 depth levels corresponding to theoretical investigation depths of 0.7 m and 1.4 m in the heather and forest respectively, with an orthogonal survey pattern (Chambers et al., 2002). They were measured roughly fortnightly from October 2015 to September 2016 making a total of 21 surveys.

Alongside the plot ERT surveys, 9 transect surveys were also conducted at each site during the growing season (Mid-April to end of September). The ERT measurements were carried out at each of the sites with 36 electrodes and an electrode spacing of 0.25 m and 5 depth levels corresponding to an investigation depth of 1.85 m. Electrodes were 0.22 m long, ow which 0.1m penetrated the ground. As with the plots, surveys used 6 stacks and 800 maximum voltage and a transmit time of 1000 ms. The inversion mesh size was equal to the spacing. The transects were surveyed to provide higher resolution insights of the VSM in the rooting zones of both the heather and forest because the existing resolution of the plot measurements was too coarse to adequately image the root zone anomaly, something which we wished to further investigate. This setup was chosen to focus on individual trees in the forest site, and for it to be logistically possible to do all four surveys on the same day.

Additionally, a larger transect was surveyed across the forest site to investigate the deeper subsurface under trees and to add context to the plot and smaller transect measurements. This transect was 72 m long, with a 1 m electrode spacing, and was surveyed at 9 depths with a theoretical investigation depth of 14 m. As with the smaller transects described above, the electrodes used were 0.22 m steel pegs.

After the surveys were completed, all data were pre-processed to remove erroneous measurements with anomalously high apparent resistivity values (>4000 Ωm) and high deviations of apparent resistivity (>0.5 Ωm) based on the quality index of the Syscal instrument. The filtered data were then corrected to 25 ^{o}C using the power function correction model of Besson et al. (2008)(Ma et al., 2011). Topography was incorporated during the pre-processing (from a survey of the sites using a total station when the arrays were installed). The measured resistivity data were then inverted using the standard least-squares constraint method in Geotomo Software's Res2dinv and Res3dinv.

3.3 Volumetric soil moisture estimation and analysis

Archie's law (Archie 1942) is commonly used to estimate soil moisture from electrical resistivity measurements (e.g. Zhou et al, 2001; Brunet et al, 2010; Schwartz et al, 2008). Specifically, Archie's law relates the electrical conductivity of a granular rock to its porosity, saturation and fluid conductivity.

There are several challenges in using ERT to estimate soil moisture, which still persist, even when partially mitigated using the generalised formula of Archie's law (Shah and Singh, 2005; Glover, 2010). In the use of this, there is still the requirement to estimate the m exponent parameter (which links the pore network of the material to the resistivity) and include the pore water resistivity. These parameters and variables can be obtained from field measurements (Zhou et al., 2001), lab measurements (Brunet et al., 2010), or both (Schwartz et al., 2008). Still, even with field estimation of the parameters and variables, their estimation brings uncertainty, which can be controlled through the verification of estimated soil moisture against field measured soil moisture (e.g. Brillante et al., 2015). This approach has led to it being successfully employed in visualising vegetation-water interactions in agricultural (e.g. Beff et al., 2013; Whalley et al., 2017) and natural environments (e.g. root zone soil moisture, al Hagrey, 2007; Ain-Lhout et al., 2016).

To estimate the VSM (θ_w) from the electrical resistivity surveys, we used Archie's law. From Archie's law, we have:

$$\rho = \rho_w \Phi^m {S_w}^n \qquad \text{(Equation 1)}$$

Here we use the parameters: ρ_w (pore water resistivity), ρ (bulk soil resistivity), Φ the water content, S_w the water saturation, n the porosity, and the parameter m which is an empirical fitting parameter. Using the generalised Archie's law (Shah and Singh, 2005; Glover, 2010), and assuming that the c parameter given by Shah and Singh (2005) = 1. This assumption was made as clay content in the soil was negligible (Sprenger et al. 2017), so the c parameter was likely to be around 1. Additionally, Shah and Singh (2005) suggest a high degree of uncertainty in c with low clay contents. We can also assume that m=n, which produces:

$$\rho = \rho_w (\Phi S_w)^m \qquad \text{(Equation 2)}$$

And thus,

$$\rho = \rho_w(\theta_w)^m \qquad \text{(Equation 3)}$$

This can then be re-arranged to give VSM (θ_w) (Equation 4).

$$\theta_w = \left(\frac{\rho_w}{\rho}\right)^{\frac{1}{m}} \qquad \text{(Equation 4)}$$

Equation 4 includes the variables: In this study, the bulk resistivity is the inverted data from the electrical resistivity tomography measurements (See section 3.2), and the pore water resistivity and the m exponent were both estimated using field data (equations 2 and 3 respectively).

During the study period, there were infrequent measurements of the pore water resistivity, however, after a large storm in January 2016, some measurements were taken at the forest site on the 8th January from the upper 15 cm of the soil profile. Two samples were taken using MicroRhizon samplers (Rhizosphere Research Products) and were analysed in the lab using a conductivity meter (Jenway Model 4510). These measurements showed the average pore water resistivity to be 350 Ωm. We then used this measured pore water resistivity (ρ_w) to calibrate m exponent, again by re-arranging the generalised Archie's law to give Equation 5.

$$m = \frac{\log(\frac{\rho_w}{\rho})}{\log \theta_w} \qquad \text{(Equation 5)}$$

The bulk resistivity (ρ_w) and VSM (θ_w) are the average measured resistivity and TDR measured soil moisture over the 0 to 0.5 m depths, respectively. We assumed the pore water resistivity to be the same at both sites, however, the bulk resistivity and the VSM differed between the heather and forest site, and as such, site specific calibrations of the m exponent were carried out. At the heather site, the average bulk resistivity was 820 Ωm and the average VSM 0.44 m^3 m^{-3}, which gave a m exponent of 1.04. At the forest site, the average bulk resistivity at 0.1-0.5 m depths was 790 Ωm and the average VSM over that depth was 0.48 m^3 m^{-3}. This gave an m exponent of 1.10. These values were then used as fixed parameters for all surveys, and are within the range of typical m exponents from the standard Archie's law formulation (between 1.0 and 2.5) (Vereecken et al., 2006). Lower m exponents indicate high connectivity of pore water. While the values estimated here might appear low, a study by Moreno et al., (2015) found root zone m exponents of around 1.06 when the m exponent was estimated using field data.

Equation 4 requires the pore water resistivity for every survey date. As this was only measured on the 8th January, we estimated it using Equation 6 (a further rearrangement of the generalized Archie's law), which required: the m exponents calculated above; the average measured VSM (θ_w) at 0.1 and 0.5 m depths from the two TDR sensors at those depths; and the bulk resistivity (ρ) from each plot survey at the same 0.1 or 0.5 m depths.

$$\rho_w = \rho {\theta_w}^m \quad \text{(Equation 6)}$$

The estimated pore water resistivities were mostly within the ranges of input waters (243-910 Ωm) and drainage waters (164-500 Ωm), with variability linked to the movement of groundwater through the profile at the flatter heather site and fast draining of input waters at the forest site due to the rockier subsurface (Fig 3).

The VSM for each of the plot surveys was then calculated using Equation 4; with the calibrated exponent (m) and the calibrated pore water resistivities (ρ_w) for each survey (as calculated above). The VSM was interpolated from the resistivity data, and selected for 0.1 and 0.5 m depths, using the surveyed bulk resistivity at those depths. The 0.1 and 0.5 m depths were chosen as they encompass the whole typical root depth range of heather (*C. vulgaris*; 0.28 m) and Scots Pine (*P. sylvestris*; 0.48 m) (Jackson et al., 1996).

The method for estimating VSM for the 8.75 m transects was identical to that of the plots, including the same pore water resistivities and m exponent. Transect VSM was estimated from the surface to 0.5 m deep, with the depth limit of 0.5 m chosen because this depth encompassed the rooting zones of both heather and forest (Fig 4). The same depth limits were applied to the heather site for purposes of comparison.

Though the methods employed require TDR measured VSMs to estimate the ERT VSM, we tested both data sets for statistical differences using the Wilcoxon signed-rank test. This test was chosen as a non-parametric version of the paired t-test, and was required as both data sets are dependent. To assess the spatio-temporal variability of VSM, we calculated statistical variance across all of the surveys for both the heather and forest plots. This highlighted the areas in the plots where the soil moisture was more susceptible to change. To compliment this, and identify areas in the plots where there was pronounced wetting and drying, we calculated the spatio-temporal ranges of VSM. We then separated these into the variance and ranges for the growing (Mid-April to end of September) and non-growing season. The same methods employed for the plot surveys was also carried out on the 8.75 m transects for the full 0-0.5 m depth.

Correlations between the spatial patterns in temporal variability and ranges were then investigated with relation to the vegetation structure in the forest site using Spearman’s correlation. Correlations between VSM and vegetation structure at the heather site were not carried out as the heather site was fairly uniform in canopy cover.

4. Results

4.1 Hydroclimate dynamics

During the study period, which ran from October 2015 to September 2016, there was 1334 mm precipitation (Fig 5a), including a very wet December and early January which contributed 507 mm to the overall total. Runoff during the period was 663 mm (though likely to be higher due to the uncertainty surrounding the storm period) and 402 mm PET. Long term average air temperature during the period was 6.8°C. Along with the January storm, there were several hydrologically interesting periods. Autumn 2015 was relatively dry, with lower than average rain fall. This was followed by an exceptionally wet winter, with a large storm on 30th December, which caused widespread flooding (Soulsby et al., 2017). Anomalously wet conditions persisted through January 2016. During this period, the regional precipitation total was 228% of the average winter precipitation total. Subsequently, February was much drier. Spring 2016 was also relatively dry with only 84% of the long-term average rainfall. The summer of 2016 was punctuated by large frontal precipitation events, and was initially wet at the beginning, becoming drier towards the end, with particularly dry spells in August and September (Fig 5a). The seasonal descriptions are from http://www.metoffice.gov.uk/climate/uk/summaries.

Potential evapotranspiration over the period followed a seasonal cycle (Fig 5a), with low evapotranspiration amounts (between 0-1 mm d^{-1}) and reduced variability in winter. Rates were higher during the summer, with increased variability. The growing season's potential evapotranspiration range was 4.4 mm per day (mean: 1.8mm), and the non-growing season range was 2.0 mm (mean: 0.4 mm). Evapotranspiration was around 70% of the precipitation input in the forest site, and 55% of the total precipitation input in the heather site (Sprenger et al., 2017; Wang et al., 2017).

4.2 Volumetric soil moisture estimation at the plot sites.

At the heather site, the average TDR measured VSM was 0.36 m^3 m^{-3}, with a standard deviation of 0.04 m^3 m^{-3} (Table 1). In comparison, the VSM estimated for the whole period using the ERT measurements was 0.35 m^3 m^{-3} (Fig 5b). The wettest period for both the TDR and ERT VSM was the January 2016 storm event. During the storm, the ERT-based VSM estimates were substantially higher than the TDR VSM measurements (0.59 m^3 m^{-3} versus 0.42 m^3 m^{-3}, respectively). Apart from the storm event, the interquartile range of ERT derived VSM in the heather plot was fairly constant. Overall, the estimated VSM using the geophysics were generally consistent with the TDR measurements, and captured the dynamics well (Fig 5b), with the Wilcoxon signed-rank test at the heather site showing no statistical significant difference (p-value =<0.058). However, the forest site unsurprisingly did show a significant difference (p-value =<0.01).

At the forest site, the average TDR measured VSM was 0.46 m^3 m^{-3}, with a standard deviation of 0.06 m^3 m^{-3} (Table 1). In comparison, the VSM estimated for the whole period from the ERT was 0.38 m^3 m^{-3} (Fig 5c). As in the heather site, the wettest period for both the TDR and ERT VSM was the January storm event. Again, during that storm, the ERT VSM was higher than the TDR VSM (0.64 m^3 m^{-3} versus 0.55 m^3 m^{-3}, respectively). The estimated VSM using the geophysics exhibited a larger systematic shift with TDR generated VSM time series than at the heather site, though still reproducing the ERT dynamics well (Fig 5c)The interquartile ranges of the VSM in the forest plot was fairly heterogeneous, with the VSM ranges largest during the wettest periods (Fig 5c).

Figures 6 and 7 show examples for wetting (17/11/15 – 08/01/16) and drying cycles (25/07/16 – 23/08/16) in the 3D ERT plots at 0.1 and 0.5 m. The dates were selected as they represented the greatest wetting and drying during the study period, with 526 mm of rain during the wetting period, and only 55 mm of precipitation during the period of drying. For the heather site at 0.1 m depth, there was a zone of high VSM through the middle of the plot during all surveys. This expanded substantially during the wetting period (Fig. 6a). During drying, VSM ranged from 0.2 to 0.6 m^3 m^{-3} on the 25/07/16 to a 0.2 to 0.5 m^3 m^{-3} on the 23/08/16 (Fig 7a). The western side, north east, and south east corners of the plots were drier, with VSM ranging of 0.2-0.5 m^3 m^{-3} during both wetting (Fig 6a) and drying periods (Fig 7a) at 0.1 m. At 0.5 m, there was fairly similar VSM content between wetting (Fig 6b) and drying (Fig 7b), though after the January storm, VSM increased substantially.

At the forest site, VSM patterns during wetting and drying had a comparatively more heterogeneous pattern (Fig 6c and d; Fig 7c and d). The areas of highest mean VSM change were roughly correlated (Average correlation coefficient of 0.3, p-value <0.01) with the areas of reduced canopy cover, with the areas of greatest change during drying being around trees (Fig 7c). This is especially clear with the tree at 2 x 5.5 m. The VSM at 0.1 m increased during wetting, ranging from 0.2 to 0.7 m^3 m^{-3} on 17/11/15 to 0.2 to 0.8 m^3 m^{-3} on the 08/01/16 (Fig 6c). During the drying period, there was general drying across the whole plot at 0.1 m (Fig 7c). Unlike the heather plot, at 0.5 m depths there was a slight increase in VSM (Fig 7d). This was probably due to wetting fronts moving down through the profile from early August rain.

4.3 Spatio-temporal heterogeneity in plot volumetric VSM

At the heather site (Fig 8a), the statistical variance of the ERT VSM showed contrasts, with variances ranging from 0 to 0.01 $(m^3\ m^{-3})^2$. With the area of highest variability roughly correlating (r= 0.45, p-value = <0.01) with the wettest locations in the plot (Fig 6a, 7a, and 8a). In the forest site, the temporal variance in the spatial domain volumetric VSM was more homogeneous than at heather site (Fig 8a versus 8b), ranging from 0 to 0.005 $(m^3\ m^{-3})^2$ (Fig 8b), with the most variable areas in the spatial domain mostly located near trees in the north and east areas of the plot (c.f. Fig 2). Ranges of soil moisture were larger at the heather site (Fig 8a), with the highest ranges also centred on the wettest parts of the plot. Ranges of around 0.2 m^3 m^{-3} were located near the trees at the forest site, with the smallest ranges located at the south-west corner of the plot in the area with least canopy cover (Fig 8b).

The variance VSM was then investigated for the growing (Mid-April to end of September) and non-growing season at the 0.1 m depth slices from the plot surveys (Fig 9). At the heather site (Fig 9a), there were striking differences in the patterns of VSM during both seasons. During the growing season, the spatial variance in VSM temporal changes were low, with variance between 0 and 0.001 (m^3 m^{-3})^2. In the non-growing season VSM variance was much more variable and higher (ranging from 0.002 to 0.01 (m^3 m^{-3})^2). At the forest site (Fig 9b), spatial patterns of VSM temporal variance were much more homogeneous than the heather site, spanning a range of 0 – 0.005 (m^3 m^{-3})^{2}in both seasons. There were however subtle differences between the non-growing and growing seasons, with the growing season having the higher variance in VSM, and in particular. The variances were highest in areas where there were trees.

4.4 Using high spatial resolution transect measurements to investigate root zone soil moisture

The transect in the forest was sited to encompass the root zone extent of two established Scots Pine trees. The transect data showed again that at the heather site, VSM variances were mostly low at all depths, though there were some VSM variances of 0.01 (m^3 m^{-3})^2 close to the surface (>0.3 m deep) (Fig 10a). The ranges of VSM also fairly low, mostly 0 - 0.2 m^3 m^{-3}, but with some ranges of 0.3 to 0.5 m^3 m^{-3}. In both plots of VSM variance and range, there was a defined boundary at 0.25 - 0.3 m where variance and range in VSM decreased substantially (Fig 11a). At the forest site, the VSM variance ranged from 0 to 0.01 (m^3 m^{-3})^2, and was generally much more heterogeneous than the heather site (Fig 10b), as a consequence of the high resistivity scree underlying the forest site (see also Fig 4). As shown for the plots in Figures 8 and 9, the greatest heterogeneity in variance and range of VSM occurred during the growing season at the forest site, with VSM ranges in upper 0.5 m of 0.1 to 0.5 m^3 m^{-3}; Fig 11b). After 0.50 m, the range generally decreased to 0 to 0.15 m^3 m^{-3}. Overall, the greatest variability with depth occurred within the root zone and was centred around the two trees (Fig 10b and Fig 11b).

5. Discussion

5.1 Estimating plot scale soil moisture from repeat plot scale ERT measurements

The approach of using plot scale ERT measurements to estimate soil moisture was able to capture the temporal patterns in VSM dynamics such as drying and wetting, at both sites, though the degree of change differed between sites. Though this could have been linked to the electrical properties of the thin peat layer at both sites, the soils at both studies sites are minerogenic, with much of the organic horizon comprising of litter. As such, the differences in the electrical properties of the thin peat layer are likely unimportant when you take into account the greater depth of minerogenic material. It is more likely, that this difference in correspondence between the ERT VSM and the TDR VSM between the heather and forest site is linked either to: (a) the greater subsurface heterogeneity at the forest site caused by the tree roots and much rockier sub-soil influencing the soil physical properties, which leads to higher heterogeneity in the resistivity of the subsurface. Or, (b) preferential flow paths which are very common in forest soils (Sidle et al., 2001), and influence the ERT results, but are not picked up by the point TDR measurements. Something also found by Hubner et al. (2015). It could also be linked to the sampling occasions of the ERT surveys integrating the larger scale heterogeneity of the subsurface (something which not possible when using point measurements) (Hübner et al., 2015), and the choice of electrode spacing (Rey et al., 2006), which was driven by the site characteristics. Heterogeneity in the subsurface can be in the form of tree roots, airspaces between rocks in the subsurface (Calamita et al., 2015), both of which are known to be present at the forest site. However, the generally reasonable correspondence between ERT and the TDR VSM time series (especially in the heather site) adds confidence to the usefulness of using ERT in the spatial estimation of VSM for plots scale studies. Though the temporal comparison of ERT VSM to TDR VSM was poorer at the forest site, the temporal dynamics of VSM from both methods was captured, with the same flashy VSM response to large precipitation inputs.

Using ERT to survey plot scale resistivity and estimation of VSM facilitates the enhanced collection of large spatial datasets, its visualisation, analysis and interpretation in contrast to long term point measured VSM time series (Brunet et al., 2010). This is important as it allows the synoptic visualisation of spatial patterns and temporal dynamics of VSM (Jayawickreme et al., 2008), something especially useful when comparing VSM under different vegetation types, where heterogeneity in vegetation structure might have a strong influence on VSM (D'Odorico et al., 2007).

During the January 2016 storm, both sites exhibited a poorer correspondence of the geophysically derived VSM with the TDR measured VSM. This is potentially linked to a change in soil water chemistry during the large events, something already documented in the Scottish Highlands (e.g. Jenkins 1989). The extreme volume of rainfall instigated a change in water conductivity, with the increased influence of low conductivity rainfall replacing the soil water leading to an increase of resistivity with wetness (Chambers et al., 2014; Mueller et al., 2016). The use of the measured natural water conductivity in the catchment alongside the estimation of the pore water resistivity allowed us to account for this. It is also likely that the TDR VSM was influenced by the change in conductivity during the storm period as TDR methods are also susceptible to conductivity changes (see Topp et al., 1994). As such, this suggests that the assumption of stable soil water resistivity over time may not always hold at this site (Brunet et al., 2010). For a reasonable estimation of VSM time variable conductivities need to be addressed, as carried out in this study by using TDR and ERT measurements to estimate the soil water conductivity. The storm period and the consequent drying highlight some of the limits of the approach used in this study, such as the absence of a soil water conductivity time series is ideally needed to increase the accuracy of estimated VSM, especially during highly variable hydrometer logical conditions. Specifically, the lack of year-long soil water resistivity measurements required their estimation using the TDR data. This effectively meant that the TDR data was used to estimate the soil water conductivity and the m exponent, leading to interdependence of the ERT and TDR VSM time series making statistical comparison challenging. Though based on empirical data, the uncertainty surrounding the estimation of the m exponent could also have been improved through the inclusion of more periods in which ERT and soil water measurement data overlapped. However, this was not possible during this study. For future studies, soil water resistivity measurements concurrent to the ERT surveys would be recommended.

Importantly though, the use of both 2D (transects) and 3D (plot) measurements has distinct advantages for surveying the subsurface as this allows high resolution, non-destructive (i.e. repeatable) visualisation of water distribution (Séger et al., 2009). The benefits of using plot measurements are that they allow the characterization of subsurface spatial heterogeneity in terms of location and extent, something not possible with transect measurements as the spatial patterns may not be orientated with the transect axis (Bentley and Gharibi 2004). In turn, transect measurements are the most widely applied ERT method and can be set up and surveyed quickly (Loke et al., 2013), with the major benefit of being able to rapidly extend the survey distances using "roll-along" methods (Donohue et al., 2012). We therefore integrated insights from both sampling approaches, overcoming the issues of low resolution due to electrode spacing in the plots, and avoiding the chance of missing subsurface spatial heterogeneity by only using transects.

As explained in section 3.3, using Archie's law requires either provision of data for, or estimation of, the parameters and certain variables (Singha and Gorelick, 2006). This estimation introduces significant uncertainty into the analysis (Brunet et al., 2010), and must be constrained through either laboratory (Brunet et al., 2010), or field data estimation (Moreno et al., 2015) as done here. In this study, we used the generalised form of Archie's law (Glover, 2010) for which the variables required to estimate VSM are bulk resistivity, pore water resistivity and the m exponent. Though calibration of the m expoenent is not required as values have been previously published for many substrates (Friedman, 2005; Vereecken et al., 2006), calibrating the factor based on site specific field data usually produces a much more realistic value (Moreno et al., 2015). Specifically, the m exponent is an empirical coefficient which relates porosity to the conductivity of the substrate (Friedman, 2005), typically ranging from 1.0 to 2.5 (Vereecken et al., 2006). In our study, both sites were between 1.0 and 1.1. Our low values are likely due to the high sand content in our soils (Sprenger et al., 2017), and the fact that we employed field calibration rather than the usual lab calibration, which - due to its destructive nature - may have changed the structure of the soil leading to the higher estimates due to compaction and decrease in permeability of the soil core (Moreno et al., 2015).

5.2 Differences in spatio-temporal dynamics of soil moisture between heather and forest dominated vegetation assemblages

The heather site showed low temporal (mostly seasonal) variability in both the TDR and average ERT VSM. In comparison, the forest site showed a higher, more marked temporally variable VSM response to precipitation inputs. Higher VSMs in the forest site can be attributed to higher organic content of soils (Jamison and Kroth, 1958; Sprenger et al., 2017). The larger temporal variability during the growing season at the forest site can be linked to the influence of vegetation when interception and evapotranspiration losses were higher (Ain-Lhout et al., 2016); and the greater subsurface drainage at this site (Geris et al., 2015). Subsurface drainage explains the flashy soil moisture response, which is likely linked to the coarse scree freely draining material underlying the forest site with its high porosity.

While temporal variability in the TDR and ERT VSM data highlighted differences and potential vegetation influences at both sites, the most marked differences were apparent when comparing the plots. Spatial variability of VSM in the heather site was lower than the forest site during periods of drying and wetting. That is, the VSM pattern remained relatively uniform during both the wet up and drying periods. This can be linked to the more uniform canopy (Soulsby et al., 2017), which is supported by the lack of variation in mean soil moisture change and higher net precipitation. The patterns of soil moisture were closely correlated with the areas of higher VSM variance, which is likely associated with the relationship of VSM, subsurface structure, and soil physical properties (Cosby et al., 1984; Qu et al., 2014). Future work will test this hypothesis further.

The relationship between VSM and areas of highest variability in VSM was more complex at the forest site, with non-uniform wetting and drying. This is most likely linked to external factors out with the subsurface structure, for example, the heterogeneity in canopy cover, patterns of throughfall and stemflow inputs (Buttle et al., 2014; Ma et al., 2014), the less dense vegetation canopy, and a different sub-canopy microclimate (Oren and Pataki, 2001; Lin, 2010). Work comparing spatial soil moisture patterns under forest and shrub vegetation is sparse in temperate settings, with most research carried out in semi-arid regions based mostly on point soil moisture measurements (e.g. Breshears et al., 1999). ERT has been successfully employed in comparing vegetation types; for example, Jayawickreme et al., (2008) conducted a study on the differences between forest and grass land using 2D transects. They found that forest exerted a stronger control on VSM than the grassland, as was the case with the forest site in our study. Here, reduced canopy cover and the mean change of VSM were roughly correlated (Correlation coefficient of 0.3, p-value = <0.01), with a potential link to the presence of, or rather distance from trees (e.g. Elliott et al., 1998). This link to the vegetation became even clearer in the VSM range, where the areas of largest VSM ranges corresponded to the trees and were related to the highest root density near the tree trunk (Elliott et al., 1998; al Hagrey, 2007) and the distributed point source inputs of large volumes of water through stem flow (Liang et al., 2011; Jian et al., 2014).

Comparing the growing and non-growing season mean soil moisture changes at the heather and forest sites highlighted further differences. The heather plot showed little spatial change in temporal VSM variability across the whole plot during the growing season whereas the forest was more heterogeneous, with areas of much greater VSM temporal variance near the bole of the trees. This is likely linked to the water partitioning and water use by the trees. The smaller VSM temporal variance seen at the heather plot was most likely again attributable to the subsurface structure and a likely greater variability in soil properties (though not specifically investigated) (Cosby et al., 1984; Qu et al., 2014). The low overall change, despite larger amounts of precipitation available for infiltration, highlights the link of VSM to the (more homogenous) vegetation cover, water use and deeper drainage. Wang et al., (2017), found the transpiration of heather to be around 17% less than the forest. This would impose a more marked vegetation influence on soil moisture at the forest site during drier periods (Warren, 2015). Soulsby et al. (2017) found that low intensity rainfall events had greater percentage interception losses than the larger events in the Bruntland Burn, a finding corroborated elsewhere by (Toba and Ohta, 2005). Higher VSM variance and range during the non-growing season at the heather site when compared to the forest site reflect the larger volume of precipitation inputs and subsequent drying/drainage, with a pattern that is closely linked to the aforementioned subsurface structure at the heather site. The cause for reduced variance and range in VSM at the forest site during the non-growing season could be due to the greater drainage, and distribution of water by the canopy during the period.

The surveying of transects with small electrode spacing under both the heather and forest vegetation sites during the growing season elucidated some of the findings from the 3D plot studies. The VSM variability between the transect surveys showed that both sites underwent changes in VSM (translatable to overall drying during this period). The drying at the heather site was confined to the upper 0.2 m, which corresponds to the rooting depths of heather (95% of roots are within the upper 0.2 m) (Sprenger et al., 2017). In the forest site, drying was focussed around the two individual trees and extended to 0.5 m deep, again corresponding to the likely maximum rooting depth of Scots Pine (Haria and Price, 2000). The presence of clear drying in the high resolution transects supports the inference that vegetation exerts a control on soil moisture at both sites. At the heather site (due to the higher number of individual plants), the vegetation exerts a control on spatial soil moisture patterns due to more homogenous canopy and more homogenous distribution of water. This finding is corroborated by Canton et al. (2004) whom looked at the relationship between canopy openness and soil moisture variability.

The presented data has highlighted differences in the interactions of heather and forest vegetation with soil moisture, which has implications for both land use and climate change. In Scotland, these findings are highly relevant as there are currently ongoing plans to afforest large areas of land (https://www.gov.uk/government/publications/2010-to-2015-government-policy-forests-and-woodland/2010-to-2015-government-policy-forests-and-woodland), and specifically, in the Cairngorm National Park of which the Bruntland Burn is part (http://cairngorms.co.uk/working-partnership/consultations/thebig9). This potential widespread vegetation change might change the water balance within the landscape (Geris et al., 2015), through an increase in forest leading to higher evapotranspirative losses and water deficits during the growing season. This finding is corroborated by Haria and Price (2000), whom found that ET was over 40% greater in a forest site. These changes would have significant bearing on hydrological stores and flows. Additionally, the projected shift of precipitation away from summer to the winter period (UKCP 09) has the potential to alter the feedbacks between soil moisture and vegetation water use, increasing growing season soil moisture deficits (Capell et al., 2013), given that the strongest influence vegetation has over soil moisture is during the growing season, where less precipitation will increase soil moisture deficits. Thus, our study has shown the potential heterogeneity in water sources in the soil could be subject to both major and subtle changes as a result of widespread increases in forest cover through more intensive water use, something further heightened through the potential decrease in growing season precipitation.

6. Conclusion

This work has highlighted the difference in soil moisture variability under two contrasting vegetation types, and showed the value of using ERT geophysics to help understand the influence of vegetation on VSM dynamics and patterns. The use of mixed ERT approaches (e.g. 3D and 2D surveys) helped to visualise and quantify vegetation-soil water interactions, and enabled the investigation of these interactions at different spatial scales and resolutions, something which would have been not possible using point measurements alone. The presented plot measurements allowed high resolution analysis of VSM spatially, and captured the heterogeneity associated with vegetation distribution as well as temporal dynamics. In addition, the transect measurements allowed a high-resolution analysis of effects of vegetation on VSM within the root zone.

Acknowledgements

We thank the British Atmospheric Data Centre for the provision of meteorological data. We also thank the European Research Council ERC (project GA 335910 VEWA) for funding through the VeWa project and the Leverhulme Trust for funding through PLATO (RPG-2014-016). The authors are grateful to the editorial comments of Daniele Penna and careful constructive criticism from three anonymous reviewers which help improve the paper.

References

'2010 to 2015 Government Policy: Forests and Woodland - GOV.UK'. 2017. May 5. https://www.gov.uk/government/publications/2010-to-2015-government-policy-forests-and-woodland/2010-to-2015-government-policy-forests-and-woodland.

Ain-Lhout, F., S. Boutaleb, M. C. Diaz-Barradas, J. Jauregui, and M. Zunzunegui. 2016. 'Monitoring the Evolution of Soil Moisture in Root Zone System of Argania Spinosa Using Electrical Resistivity Imaging'. *Agricultural Water Management* 164: 158–166.

Archie, G.E. 1942. 'The Electrical Resistivity Log as an Aid in Determining Some Reservoir Characteristics'. *Transactions of the AIME* 146 (1): 54–62. doi:10.2118/942054-G.

Beff, L, T Günther, B Vandoorne, V Couvreur, and M Javaux. 2013. 'Three-Dimensional Monitoring of Soil Water Content in a Maize Field Using Electrical Resistivity Tomography'. *Hydrology and Earth System Sciences* 17 (2): 595–609.

Bentley, L.R., and M Gharibi. 2004. 'Two-and Three-Dimensional Electrical Resistivity Imaging at a Heterogeneous Remediation Site'. *Geophysics* 69 (3): 674–680.

Besson, A, I. Cousin, A. Dorigny, M. Dabas, and Dominique King. 2008. 'The Temperature Correction for the Electrical Resistivity Measurements in Undisturbed Soil Samples: Analysis of the Existing Conversion Models and Proposal of a New Model'. *Soil Science* 173 (10): 707–720.

Binley, A., S.S. Hubbard, J.A. Huisman, A. Revil, D.A. Robinson, K. Singha, and L.D. Slater. "The Emergence of Hydrogeophysics for Improved Understanding of Subsurface Processes over Multiple Scales." *Water Resources Research* 51, no. 6 (2015): 3837–3866.

Birkel, C., D. Tetzlaff, S. M. Dunn, and C. Soulsby. 2010. 'Towards a Simple Dynamic Process Conceptualization in Rainfall–runoff Models Using Multi-Criteria Calibration and Tracers in

Temperate, Upland Catchments’. *Hydrological Processes* 24 (3): 260–275. doi:10.1002/hyp.7478.

Boaga, J., M. Rossi, and G. Cassiani. “Monitoring Soil-Plant Interactions in an Apple Orchard Using 3D Electrical Resistivity Tomography.” *Procedia Environmental Sciences*, Four Decades of Progress in Monitoring and Modeling of Processes in the Soil-Plant-Atmosphere System: Applications and Challenges, 19 (January 1, 2013): 394–402. doi:10.1016/j.proenv.2013.06.045.

Breshears, D.D., and F.J. Barnes. 1999. ‘Interrelationships between Plant Functional Types and Soil Moisture Heterogeneity for Semiarid Landscapes within the Grassland/forest Continuum: A Unified Conceptual Model’. *Landscape Ecology* 14 (5): 465–478.

Brillante, L., O. Mathieu, B. Bois, C. van Leeuwen, and J. Lévêque. 2015. ‘The Use of Soil Electrical Resistivity to Monitor Plant and Soil Water Relationships in Vineyards’. *SOIL* 1 (1): 273–286.

Brocca, L., T. Tullo, F. Melone, T. Moramarco, and R. Morbidelli. 2012. ‘Catchment Scale Soil Moisture Spatial–temporal Variability’. *Journal of Hydrology* 422–423 (February): 63–75. doi:10.1016/j.jhydrol.2011.12.039.

Brunet, P, R Clément, and C Bouvier. 2010. ‘Monitoring Soil Water Content and Deficit Using Electrical Resistivity Tomography (ERT) – A Case Study in the Cevennes Area, France’. *Journal of Hydrology* 380 (1–2): 146–53. doi:10.1016/j.jhydrol.2009.10.032.

Buttle, J.M., H.J. Toye, W.J. Greenwood, and R. Bialkowski. 2014. ‘Stemflow and Soil Water Recharge during Rainfall in a Red Pine Chronosequence on the Oak Ridges Moraine, Southern Ontario, Canada’. *Journal of Hydrology* 517 (September): 777–90. doi:10.1016/j.jhydrol.2014.06.014.

Calamita, G., A. Perrone, L. Brocca, B. Onorati, and S. Manfreda. 2015. ‘Field Test of a Multi-Frequency Electromagnetic Induction Sensor for Soil Moisture Monitoring in Southern Italy

Test Sites'. *Journal of Hydrology* 529 (October):316–29. https://doi.org/10.1016/j.jhydrol.2015.07.023.

Cantón, Y., A. Solé-Benet, and F. Domingo. 2004. 'Temporal and Spatial Patterns of Soil Moisture in Semiarid Badlands of SE Spain'. *Journal of Hydrology* 285 (1): 199–214. doi:10.1016/j.jhydrol.2003.08.018.

Capell, R., D. Tetzlaff, and C. Soulsby. 2013. 'Will Catchment Characteristics Moderate the Projected Effects of Climate Change on Flow Regimes in the Scottish Highlands?: Effects of climate change in catchments along a hydroclimate transect'. *Hydrological Processes* 27 (5): 687–99. doi:10.1002/hyp.9626.

Chambers, J.E., D.A. Gunn, P.B. Wilkinson, P.I. Meldrum, E. Haslam, S. Holyoake, M. Kirkham, O. Kuras, A. Merritt, and J. Wragg. 2014. '4D Electrical Resistivity Tomography Monitoring of Soil Moisture Dynamics in an Operational Railway Embankment'. *Near Surface Geophysics* 12 (2007). doi:10.3997/1873-0604.2013002.

Chambers, J., R. Ogilvy, O. Kuras, J. Cripps, and P. Meldrum. "3D Electrical Imaging of Known Targets at a Controlled Environmental Test Site." *Environmental Geology* 41, no. 6 (February 1, 2002): 690–704. doi:10.1007/s00254-001-0452-4.

Coenders-Gerrits, A. M. J., L. Hopp, H. H. G. Savenije, and L. Pfister. 2013. 'The Effect of Spatial Throughfall Patterns on Soil Moisture Patterns at the Hillslope Scale'. *Hydrol. Earth Syst. Sci* 17: 1749–1763.

Cosby, B. J., G. M. Hornberger, R. B. Clapp, and ToR Ginn. 1984. 'A Statistical Exploration of the Relationships of Soil Moisture Characteristics to the Physical Properties of Soils'. *Water Resources Research* 20 (6): 682–690.

Cosh, M.H., T.J. Jackson, R. Bindlish, and J.H. Prueger. 2004. 'Watershed Scale Temporal and Spatial Stability of Soil Moisture and Its Role in Validating Satellite Estimates'. *Remote Sensing of Environment* 92 (4): 427–35. doi:10.1016/j.rse.2004.02.016.

Dick, J. J., D. Tetzlaff, C. Birkel, and C. Soulsby. 2014. 'Modelling Landscape Controls on Dissolved Organic Carbon Sources and Fluxes to Streams'. *Biogeochemistry*, December, 1–14.

D'Odorico, P, K. Caylor, G.S. Okin, and T.M. Scanlon. 2007. 'On Soil Moisture-Vegetation Feedbacks and Their Possible Effects on the Dynamics of Dryland Ecosystems: SOIL MOISTURE-Vegetation Feedbacks'. *Journal of Geophysical Research: Biogeosciences* 112 (G4): n/a-n/a. doi:10.1029/2006JG000379.

Donohue, S, M. Long, P. O'Connor, and others. 2012. 'Multi-Method Geophysical Mapping of Quick Clay'. http://researchrepository.ucd.ie/handle/10197/4891.

Dunn, S. M., and R. Mackay. "Spatial Variation in Evapotranspiration and the Influence of Land Use on Catchment Hydrology." *Journal of Hydrology* 171, no. 1 (September 1, 1995): 49–73. doi:10.1016/0022-1694(95)02733-6.

Elliott, J. A., B. M. Toth, R. J. Granger, and J. W. Pomeroy. 1998. 'Soil Moisture Storage in Mature and Replanted Sub-Humid Boreal Forest Stands'. *Canadian Journal of Soil Science* 78 (1): 17–27. doi:10.4141/S97-021.

Entekhabi, D, I. Rodriguez-Iturbe, and F. Castelli. 1996. 'Mutual Interaction of Soil Moisture State and Atmospheric Processes'. *Journal of Hydrology* 184 (1–2): 3–17.

Ford, E. D., and J. D. Deans. 1978. 'The Effects of Canopy Structure on Stemflow, Throughfall and Interception Loss in a Young Sitka Spruce Plantation'. *Journal of Applied Ecology*, 905–917.

Friedman, S.P. 2005. ‘Soil Properties Influencing Apparent Electrical Conductivity: A Review’. *Computers and Electronics in Agriculture*, Applications of Apparent Soil Electrical Conductivity in Precision Agriculture, 46 (1–3): 45–70. doi:10.1016/j.compag.2004.11.001.

Garré, S., M. Javaux, J. Vanderborght, L. Pagès, and H. Vereecken. “Three-Dimensional Electrical Resistivity Tomography to Monitor Root Zone Water Dynamics.” *Vadose Zone Journal* 10, no. 1 (February 1, 2011): 412–24. doi:10.2136/vzj2010.0079.

Geris, J, D. Tetzlaff, J. McDonnell, and C. Soulsby. 2015. ‘The Relative Role of Soil Type and Tree Cover on Water Storage and Transmission in Northern Headwater Catchments: soil and vegetation effects on water storage and transmission’. *Hydrological Processes* 29 (7): 1844–60. doi:10.1002/hyp.10289.

Geris, J., D. Tetzlaff, and C. Soulsby. 2015. ‘Resistance and Resilience to Droughts: Hydropedological Controls on Catchment Storage and Run-off Response: Hydropedological Controls on Drought Resistance and Resilience’. *Hydrological Processes* 29 (21): 4579–93. doi:10.1002/hyp.10480.

Glover, Paul W. J. 2010. ‘A Generalized Archie’s Law for N Phases’. *GEOPHYSICS* 75 (6): E247–65. doi:10.1190/1.3509781.

Hagrey, S.A. al. 2007. ‘Geophysical Imaging of Root-Zone, Trunk, and Moisture Heterogeneity’. *Journal of Experimental Botany* 58 (4): 839–854.

Haria, A.H., and D.J. Price. 2000. ‘Evaporation from Scots Pine (Pinus Sylvestris) Following Natural Re-Colonisation of the Cairngorm Mountains, Scotland’. *Hydrology and Earth System Sciences Discussions* 4 (3): 451–461.

Hasselquist, N.J., M.F. Allen, and L.S. Santiago. 2010. ‘Water Relations of Evergreen and Drought-Deciduous Trees along a Seasonally Dry Tropical Forest Chronosequence’. *Oecologia* 164 (4): 881–90. doi:10.1007/s00442-010-1725-y.

Helvey, J, and J.H. Patric. 1965. ‘Canopy and Litter Interception of Rainfall by Hardwoods of Eastern United States’. *Water Resources Research* 1 (2): 193–206.

Hübner, R., K. Heller, T. Günther, and A. Kleber. “Monitoring Hillslope Moisture Dynamics with Surface ERT for Enhancing Spatial Significance of Hydrometric Point Measurements.” *Hydrology and Earth System Sciences* 19, no. 1 (2015): 225.

Jackson, R. B., J. Canadell, James R. Ehleringer, H. A. Mooney, O. E. Sala, and E. D. Schulze. 1996. ‘A Global Analysis of Root Distributions for Terrestrial Biomes’. *Oecologia* 108 (3): 389–411.

Jamison, V. C., and E. M. Kroth. 1958. ‘Available Moisture Storage Capacity in Relation to Textural Composition and Organic Matter Content of Several Missouri Soils’. *Soil Science Society of America Journal* 22 (3): 189–192.

Jayawickreme, D.H., R.L. Van Dam, and D.W. Hyndman. 2008. ‘Subsurface Imaging of Vegetation, Climate, and Root-Zone Moisture Interactions’. *Geophysical Research Letters* 35 (18). doi:10.1029/2008GL034690.

Jenkins, A. 1989. ‘Storm Period Hydrochemical Response in an Unforested Scottish Catchment’. *Hydrological Sciences Journal* 34 (4): 393–404.

Jian, S.Q, C. Zhao, S. Fang, and Kai Yu. 2014. ‘Characteristics of Caragana Korshinskii and Hippophae Rhamnoides Stemflow and Their Significance in Soil Moisture Enhancement in Loess Plateau, China’. *Journal of Arid Land* 6 (1): 105–116.

Liang, W, K.I. Kosugi, and T. Mizuyama. 2011. ‘Soil Water Dynamics around a Tree on a Hillslope with or without Rainwater Supplied by Stemflow: soil water dynamics with or without stemflow’. *Water Resources Research* 47 (2): n/a-n/a. doi:10.1029/2010WR009856.

Lin, B.B. 2010. ‘The Role of Agroforestry in Reducing Water Loss through Soil Evaporation and Crop Transpiration in Coffee Agroecosystems’. *Agricultural and Forest Meteorology* 150 (4): 510–518.

Loke, M.H., J.E. Chambers, D.F. Rucker, O. Kuras, and P.B. Wilkinson. 2013. ‘Recent Developments in the Direct-Current Geoelectrical Imaging Method’. *Journal of Applied Geophysics* 95 (August): 135–56. doi:10.1016/j.jappgeo.2013.02.017.

Ma, R, A. McBratney, B. Whelan, B. Minasny, and M. Short. 2011. ‘Comparing Temperature Correction Models for Soil Electrical Conductivity Measurement’. *Precision Agriculture* 12 (1): 55–66.

Ma, Y, R.L. Van Dam, and D.H. Jayawickreme. 2014. ‘Soil Moisture Variability in a Temperate Deciduous Forest: Insights from Electrical Resistivity and Throughfall Data’. *Environmental Earth Sciences* 72 (5): 1367–81. doi:10.1007/s12665-014-3362-y.

Mittelbach, Heidi, Irene Lehner, and Sonia I. Seneviratne. 2012. ‘Comparison of Four Soil Moisture Sensor Types under Field Conditions in Switzerland’. *Journal of Hydrology* 430–431 (April): 39–49. doi:10.1016/j.jhydrol.2012.01.041.

Moreno, Z, A. Arnon-Zur, and A. Furman. 2015. ‘Hydro-Geophysical Monitoring of Orchard Root Zone Dynamics in Semi-Arid Region’. *Irrigation Science* 33 (4): 303–18. doi:10.1007/s00271-015-0467-3.

Mueller, M.H., A. Alaoui, and C. Alewell. 2016. ‘Water and Solute Dynamics during Rainfall Events in Headwater Catchments in the Central Swiss Alps under the Influence of Green Alder Shrubs and Wetland Soils: Water and Solute Dynamics During Rainfall in Headwater Catchments’. *Ecohydrology* 9 (6): 950–63. doi:10.1002/eco.1692.

Murphy et al., 2009. ‘UK Climate Projections Science Report: Climate Change Projections’. Exeter: Met Office Hadley Centre.

‘National Park Partnership Plan 2017-2022: Consultation - Cairngorms National Park AuthorityCairngorms National Park Authority’. 2017. May 5. http://cairngorms.co.uk/working-partnership/consultations/thebig9/.

Oren, R, and D.E. Pataki. 2001. ‘Transpiration in Response to Variation in Microclimate and Soil Moisture in Southeastern Deciduous Forests’. *Oecologia* 127 (4): 549–559.

Peterson, A.M., W.D. Helgason, and A.M. Ireson. 2016. ‘Estimating Field-Scale Root Zone Soil Moisture Using the Cosmic-Ray Neutron Probe’. *Hydrology and Earth System Sciences* 20 (4): 1373–85. doi:10.5194/hess-20-1373-2016.

Porporato, A, E. Daly, and I. Rodriguez-Iturbe. 2004. ‘Soil Water Balance and Ecosystem Response to Climate Change’. *The American Naturalist* 164 (5): 625–32. doi:10.1086/424970.

Pypker, T.G., B.J. Bond, T.E. Link, D. Marks, and M.H. Unsworth. 2005. ‘The Importance of Canopy Structure in Controlling the Interception Loss of Rainfall: Examples from a Young and an Old-Growth Douglas-Fir Forest’. *Agricultural and Forest Meteorology* 130 (1): 113–129.

Qu, W., H. R. Bogena, J. A. Huisman, G. Martinez, Y. A. Pachepsky, and H. Vereecken. 2014. ‘Effects of Soil Hydraulic Properties on the Spatial Variability of Soil Water Content: Evidence from Sensor Network Data and Inverse Modeling’. *Vadose Zone Journal* 13 (12): 0. doi:10.2136/vzj2014.07.0099.

Rey, E, D. Jongmans, P. Gotteland, and S. Garambois. 2006. ‘Characterisation of Soils with Stony Inclusions Using Geoelectrical Measurements’. *Journal of Applied Geophysics* 58 (3): 188–201. doi:10.1016/j.jappgeo.2005.06.003.

Reyer, C.P.O., S. Leuzinger, A. Rammig, Annett Wolf, Ruud P. Bartholomeus, Antonello Bonfante, Francesca de Lorenzi, et al., 2013. ‘A Plant’s Perspective of Extremes: Terrestrial Plant Responses to Changing Climatic Variability’. *Global Change Biology* 19 (1): 75–89. doi:10.1111/gcb.12023.

Rigling, A, C. Bigler, B. Eilmann, E. Feldmeyer-Christe, U. Gimmi, C. Ginzler, U. Graf, et al., 2013. ‘Driving Factors of a Vegetation Shift from Scots Pine to Pubescent Oak in Dry Alpine Forests’. *Global Change Biology* 19 (1): 229–40. doi:10.1111/gcb.12038.

Robinson, D. A., A. Binley, N. Crook, F. D. Day-Lewis, T. P. A. Ferré, V. J. S. Grauch, R. Knight, et al., 2008. 'Advancing Process-Based Watershed Hydrological Research Using near-Surface Geophysics: A Vision For, and Review Of, Electrical and Magnetic Geophysical Methods'. *Hydrological Processes* 22 (August): 3604–35. doi:10.1002/hyp.6963.

Rodriguez-Iturbe, I., P. D'Odorico, A. Porporato, and L. Ridolfi. 1999. 'On the Spatial and Temporal Links between Vegetation, Climate, and Soil Moisture'. *Water Resources Research* 35 (12): 3709–22. doi:10.1029/1999WR900255.

Rodríguez-Iturbe, I, and A. Porporato. 2007. *Ecohydrology of Water-Controlled Ecosystems: Soil Moisture and Plant Dynamics*. Cambridge University Press.

Schwartz, B.F., M.E. Schreiber, and T. Yan. 2008. 'Quantifying Field-Scale Soil Moisture Using Electrical Resistivity Imaging'. *Journal of Hydrology* 362 (3–4): 234–46. doi:10.1016/j.jhydrol.2008.08.027.

Séger, M., I. Cousin, A. Frison, H. Boizard, and G. Richard. 2009. 'Characterisation of the Structural Heterogeneity of the Soil Tilled Layer by Using in Situ 2D and 3D Electrical Resistivity Measurements'. *Soil and Tillage Research* 103 (2): 387–398.

Seneviratne, S.I., T. Corti, E.L. Davin, M. Hirschi, E.B. Jaeger, I. Lehner, B. Orlowsky, and A. J. Teuling. 2010. 'Investigating Soil Moisture–climate Interactions in a Changing Climate: A Review'. *Earth-Science Reviews* 99 (3–4): 125–61. doi:10.1016/j.earscirev.2010.02.004.

Shah, P.H., and D. N. Singh. "Generalized Archie's Law for Estimation of Soil Electrical Conductivity." *Journal of ASTM International* 2, no. 5 (2005): 1–20.

Sidle, R.C., S. Noguchi, Y. Tsuboyama, and K. Laursen. 2001. 'A Conceptual Model of Preferential Flow Systems in Forested Hillslopes: Evidence of Self-Organization'. *Hydrological Processes* 15 (10):1675–92. https://doi.org/10.1002/hyp.233.

Singha, K, and S.M. Gorelick. 2006. 'Effects of Spatially Variable Resolution on Field-Scale Estimates of Tracer Concentration from Electrical Inversions Using Archie's Law'. *GEOPHYSICS* 71 (3): G83–91. doi:10.1190/1.2194900.

Soulsby, C., C. Birkel, J. Geris, J. Dick, C. Tunaley, and D. Tetzlaff. 2015. 'Stream Water Age Distributions Controlled by Storage Dynamics and Nonlinear Hydrologic Connectivity: Modelling with High-Resolution Isotope Data: stream water age controlled by storage and connectivity'. *Water Resources Research* 51 (9): 7759–76. doi:10.1002/2015WR017888.

Soulsby, C., J. Dick, B. Scheliga, and D. Tetzlaff. 2017. 'Taming the Flood - How Far Can We Go with Trees?' *Hydrological Processes*, May. doi:10.1002/hyp.11226.

Soulsby, C., J. Bradford, J. Dick, J. P. McNamara, J. Geris, J. Lessels, M. Blumstock, and D. Tetzlaff. 2016. 'Using Geophysical Surveys to Test Tracer-Based Storage Estimates in Headwater Catchments.: Geophysical Surveys to Test Tracer-Based Storage Estimates'. *Hydrological Processes*, April. doi:10.1002/hyp.10889.

Soulsby, C., D. Tetzlaff, N. van den Bedem, I.A. Malcolm, P.J. Bacon, and A.F. Youngson. 2007. 'Inferring Groundwater Influences on Surface Water in Montane Catchments from Hydrochemical Surveys of Springs and Streamwaters'. *Journal of Hydrology* 333 (2–4): 199–213. doi:10.1016/j.jhydrol.2006.08.016.

Soulsby, C., H. Braun, M. Sprenger, M. Weiler, and D. Tetzlaff. "Influence of Forest and Shrub Canopies on Precipitation Partitioning and Isotopic Signatures." *Hydrological Processes*, n.d., n/a-n/a. doi:10.1002/hyp.11351.

Sprenger, M, D. Tetzlaff, and C. Soulsby. 2017. 'Stable Isotopes Reveal Evaporation Dynamics at the Soil-Plant-Atmosphere Interface of the Critical Zone'. *Hydrology and Earth System Sciences Discussions*, February, 1–37. doi:10.5194/hess-2017-87.

Stephenson, N.L. 1990. ‘Climatic Control of Vegetation Distribution: The Role of the Water Balance’. *The American Naturalist* 135 (5): 649–670.

Stewart, G, and A. C. Hull. 1949. ‘Cheatgrass (Bromus Tectorum L.)--An Ecologic Intruder in Southern Idaho’. *Ecology* 30 (1): 58–74. doi:10.2307/1932277.

Srayeddin, I., and C. Doussan. “Estimation of the Spatial Variability of Root Water Uptake of Maize and Sorghum at the Field Scale by Electrical Resistivity Tomography.” *Plant and Soil* 319, no. 1–2 (2009): 185–207.

Tetzlaff, D, C. Birkel, J. Dick, J. Geris, and C. Soulsby. 2014. ‘Storage Dynamics in Hydropedological Units Control Hillslope Connectivity, Runoff Generation, and the Evolution of Catchment Transit Time Distributions’. *Water Resources Research* 50 (2): 969–985.

Teuling, A.J., R. Uijlenhoet, F. Hupet, and P.A. Troch. 2006. ‘Impact of Plant Water Uptake Strategy on Soil Moisture and Evapotranspiration Dynamics during Drydown’. *Geophysical Research Letters* 33 (3). doi:10.1029/2005GL025019.

Toba, T., and T. Ohta. 2005. ‘An Observational Study of the Factors That Influence Interception Loss in Boreal and Temperate Forests’. *Journal of Hydrology* 313 (3): 208–220.

Tomaškovičová, S., T. Ingeman-Nielsen, A. Christiansen, I. Brandt, T. Dahlin, and B. Elberling. “Effect of Electrode Shape on Grounding Resistances — Part 2: Experimental Results and Cryospheric Monitoring.” *GEOPHYSICS* 81, no. 1 (January 1, 2016): WA169-WA182. doi:10.1190/geo2015-0148.1.

Topp, G. C., S. J. Zegelin, and I. White. 1994. ‘Monitoring Soil Water Content Using TDR: An Overview of Progress’. In *Proc. Symp. Workshop Time Domain Reflectometry Environ., Infrastructure, Mining Appl.*, 67–80. https://publications.csiro.au/rpr/pub?list=BRO&pid=procite:b202617e-44da-4ac8-849f-2211a581609b.

Vereecken, H., J. A. Huisman, H. Bogena, J. Vanderborght, J. A. Vrugt, and J. W. Hopmans. 2008. 'On the Value of Soil Moisture Measurements in Vadose Zone Hydrology: A Review: SOIL MOISTURE AND HYDROLOGY'. *Water Resources Research* 44 (4): n/a-n/a. doi:10.1029/2008WR006829.

Vereecken, H, A. Binley, G. Cassiani, A. Revil, and K. Titov. 2006. 'APPLIED HYDROGEOPHYSICS'. In *Applied Hydrogeophysics*, 71:1–8. Dordrecht: Springer Netherlands. http://link.springer.com/10.1007/978-1-4020-4912-5_1.

Wang, H, D. Tetzlaff, J.J. Dick, and C. Soulsby. 2017. 'Assessing the Environmental Controls on Scots Pine Transpiration and the Implications for Water Partitioning in a Boreal Headwater Catchment'. *Agricultural and Forest Meteorology* 240: 58–66.

Warren, R.K. 2015. 'Examining the Spatial Distribution of Soil Moisture and Its Relationship to Vegetation and Permafrost Dynamics in a Subarctic Permafrost Peatland'.

Whalley, William R., A. Binley, C. W. Watts, Peter Shanahan, Ian Charles Dodd, E. S. Ober, R. W. Ashton, C. P. Webster, R. P. White, and Malcolm J. Hawkesford. "Methods to Estimate Changes in Soil Water for Phenotyping Root Activity in the Field." *Plant and Soil*, 2017, 1–16.

Zhou, Q.Y., J. Shimada, and A. Sato. 2001. 'Three-Dimensional Spatial and Temporal Monitoring of Soil Water Content Using Electrical Resistivity Tomography'. *Water Resources Research* 37 (2): 273–85. doi:10.1029/2000WR900284.

Zonge, K., J. Wynn, and S. Urquhart. "9. Resistivity, Induced Polarization, and Complex Resistivity." In *Near-Surface Geophysics*, 265–300. Investigations in Geophysics. Society of Exploration Geophysicists, 2005. doi:10.1190/1.9781560801719.ch9.

Zreda, M, D. Desilets, T. P. A. Ferré, and Russell L. Scott. 2008. 'Measuring Soil Moisture Content Non-Invasively at Intermediate Spatial Scale Using Cosmic-Ray Neutrons'. *Geophysical Research Letters* 35 (21). http://onlinelibrary.wiley.com/doi/10.1029/2008GL035655/full.

Zribi, M, T. Paris Anguela, B. Duchemin, Z. Lili, W. Wagner, S. Hasenauer, and Abdelghani Chehbouni. 2010. 'Relationship between Soil Moisture and Vegetation in the Kairouan Plain Region of Tunisia Using Low Spatial Resolution Satellite Data'. *Water Resources Research* 46 (6). http://onlinelibrary.wiley.com/doi/10.1029/2009WR008196/full.

Tables

	Mean ($m^3\ m^{-3}$)	Coefficient of variation ($m^3\ m^{-3}$)
Heather	0.36	0.11
Forest	0.46	0.12

Table 1: Average and coefficient of variation of VSM measured using TDR probes during study period

Figures

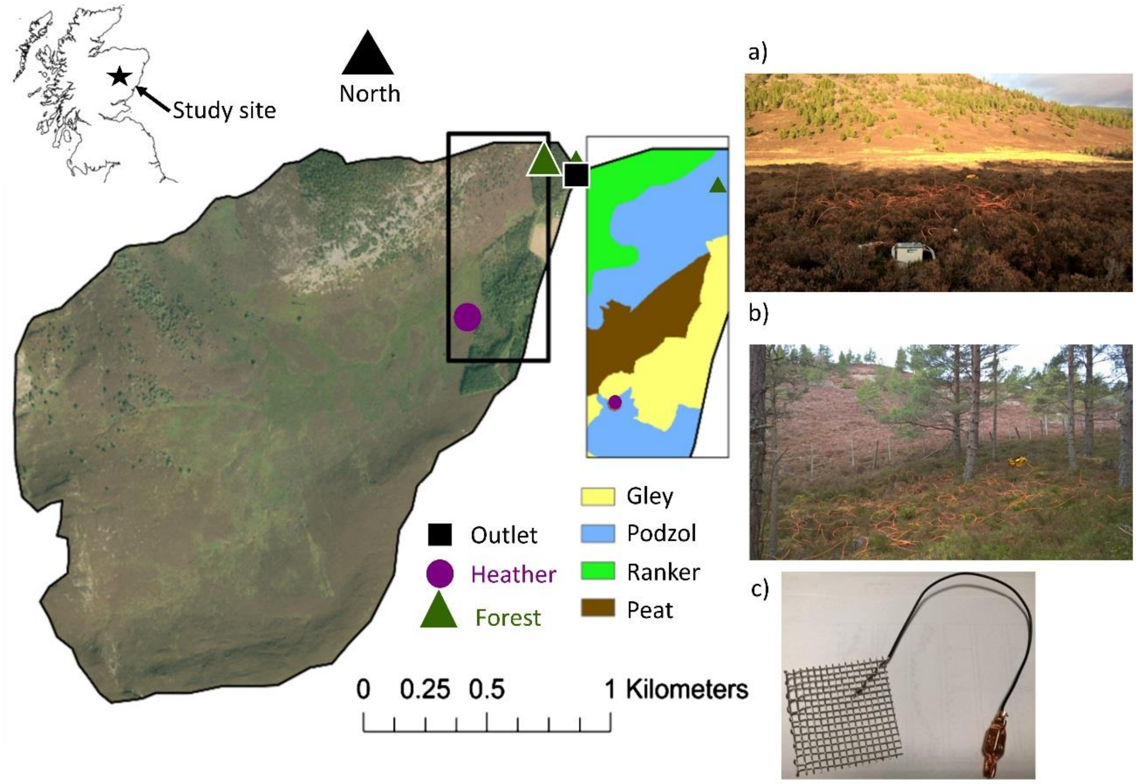

Fig. 1: Aerial image (1:12000) of Bruntland Burn catchment showing the heather and forest study sites, and catchment outlet. Map insert (1:8500) shows soil type of the study sites. Inset photographs show the field setting for the plots in the heather (a) and forest sites (b), respectively. Photography c, shows the electrode design (5x5 cm).

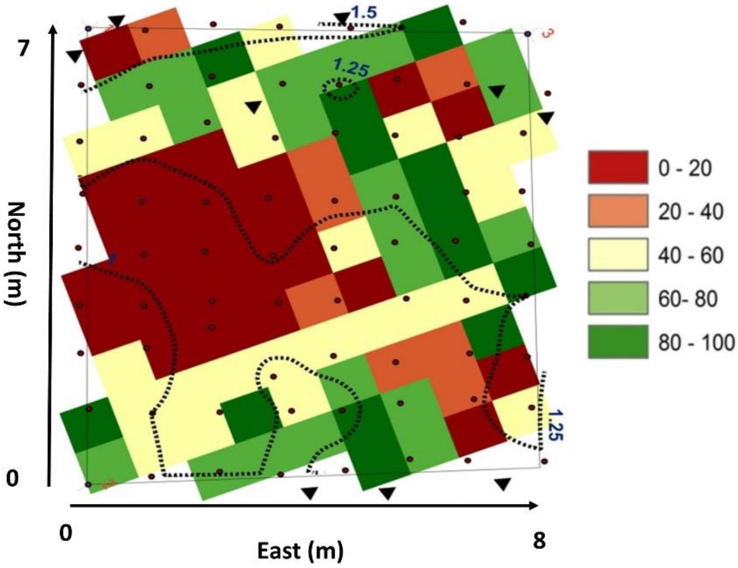

Fig. 2: Canopy cover (in %) and elevation (contour intervals: 0.25 m) relative to point (0, 0) for the forest site. Black triangles indicate tree locations.

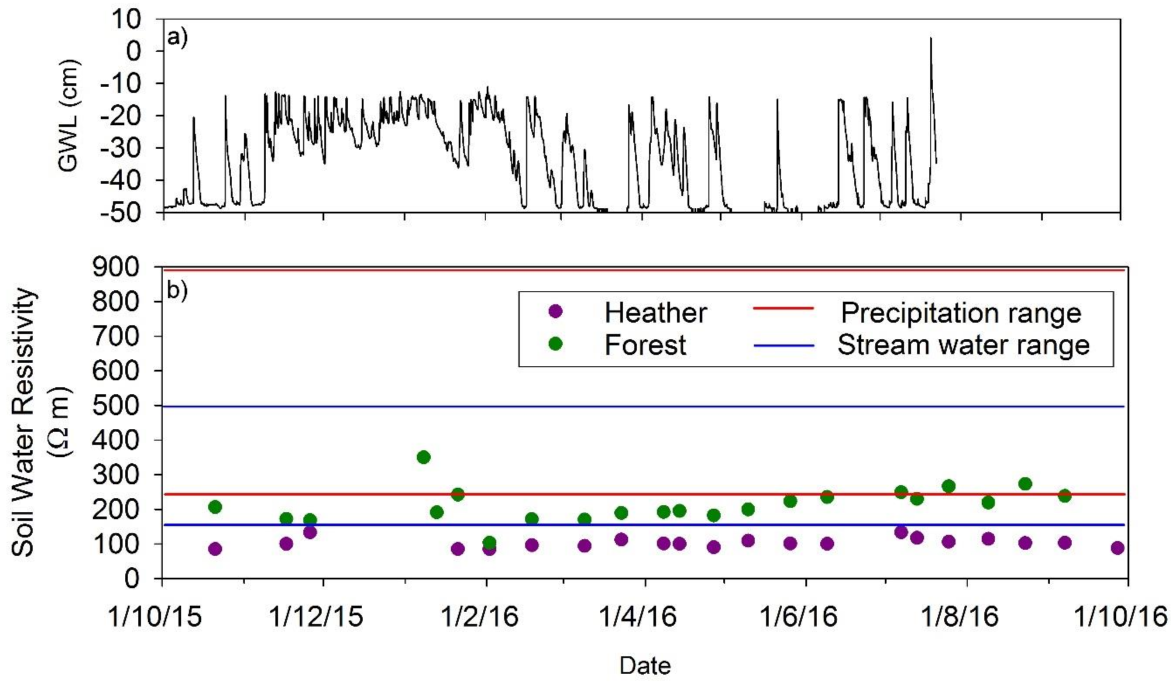

Fig. 3: a) Groundwater level (GWL) for the heather site, and b) estimated soil water resistivity values for each survey at the heather and forest site. Lines indicate the measured precipitation and stream water resistivity. Groundwater time-series at the heather site ends in late July due to logger failure.

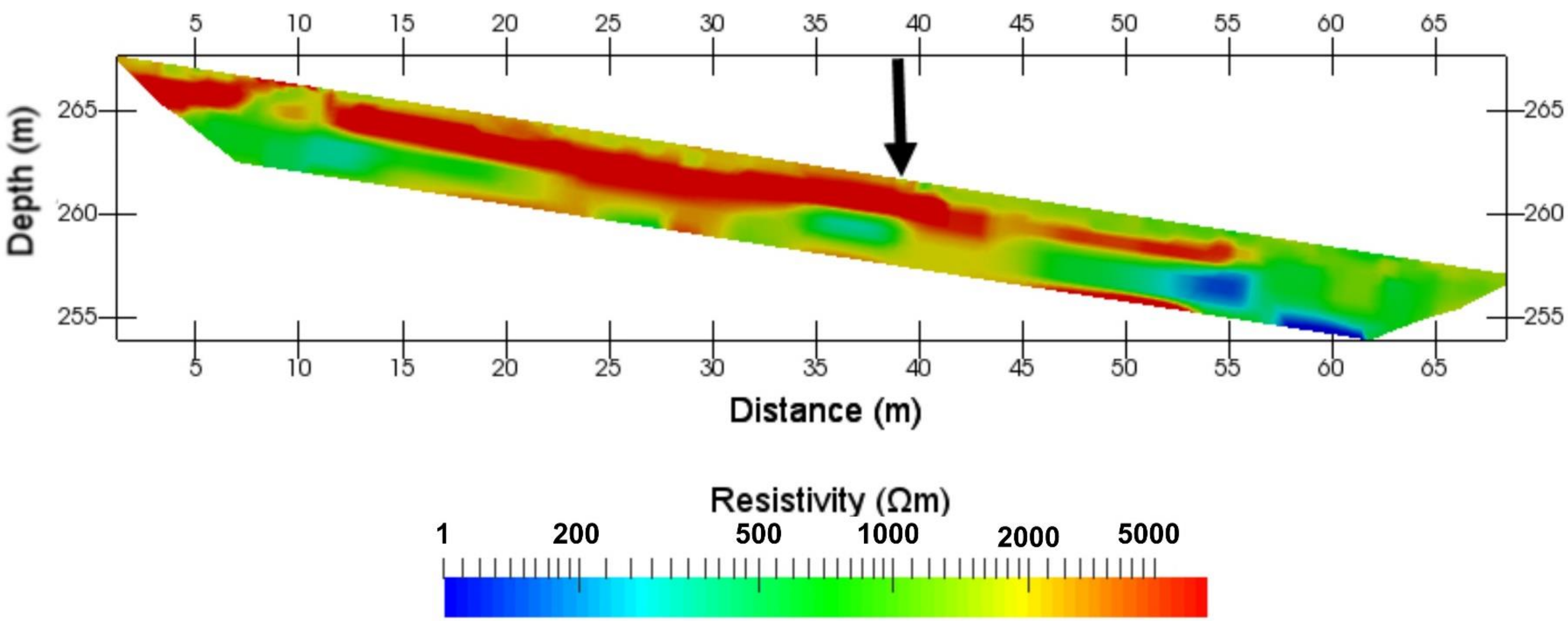

Fig. 4: Resistivity for the 72 m long transect through the forest hillslope, showing high resistivity scree material in the shallow subsurface. Black arrow indicates location of plot and transect.

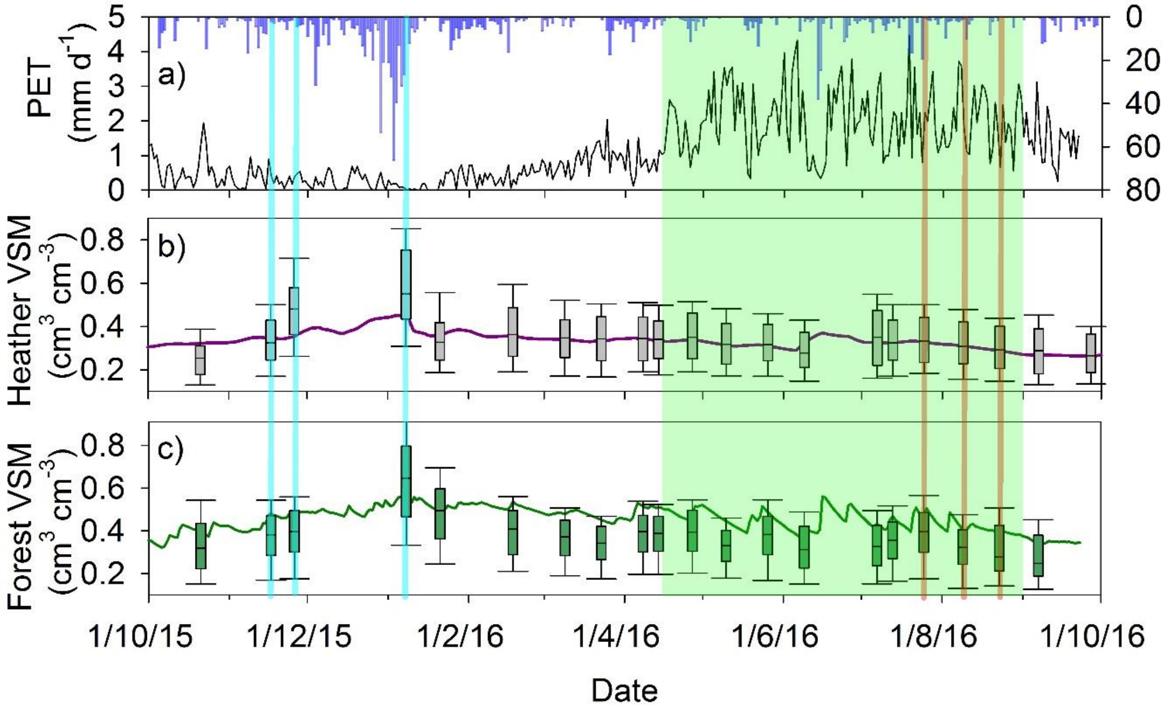

Fig. 5: Time series of: a) precipitation (P) and potential evapotranspiration (PET), b) VSM at the heather site, and c) VSM at the forest site. Solid lines in b and c represent the TDR measured VSM, and the box plots represent the mean, 5th, 25th, 75th, and 95th percentiles. Additionally, the blue and orange lines represent the periods of wetting and drying in Figure 7 respectively, and the green shading, the growing season.

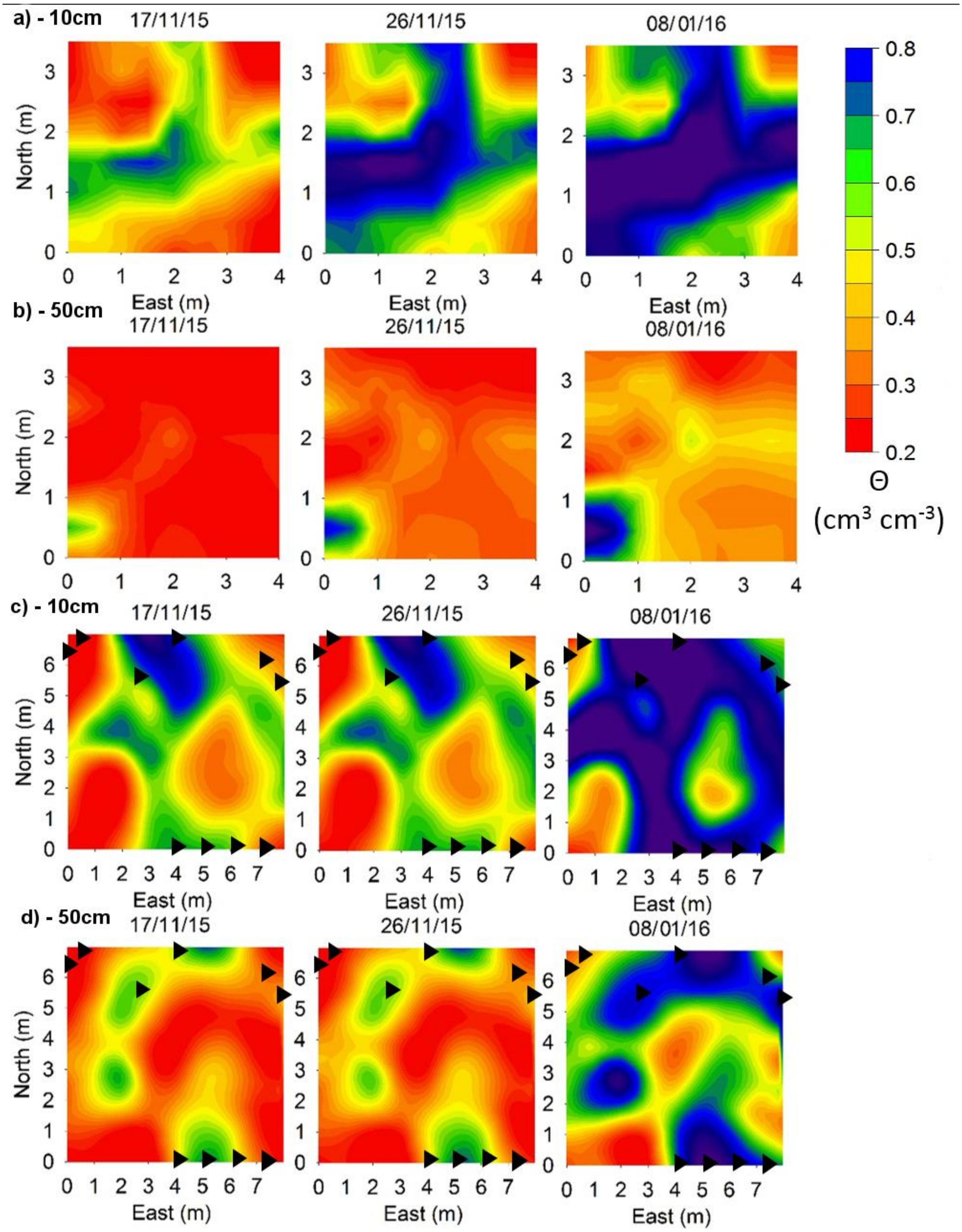

Fig. 6: Wetting cycle from 17/11/15 to 08/01/16 at the heather sites 0.1 m (a) and 0.5 m (b) depths, and the forest sites 0.1 m (c) and 0.5 m (d) depths. Black triangles are tree locations.

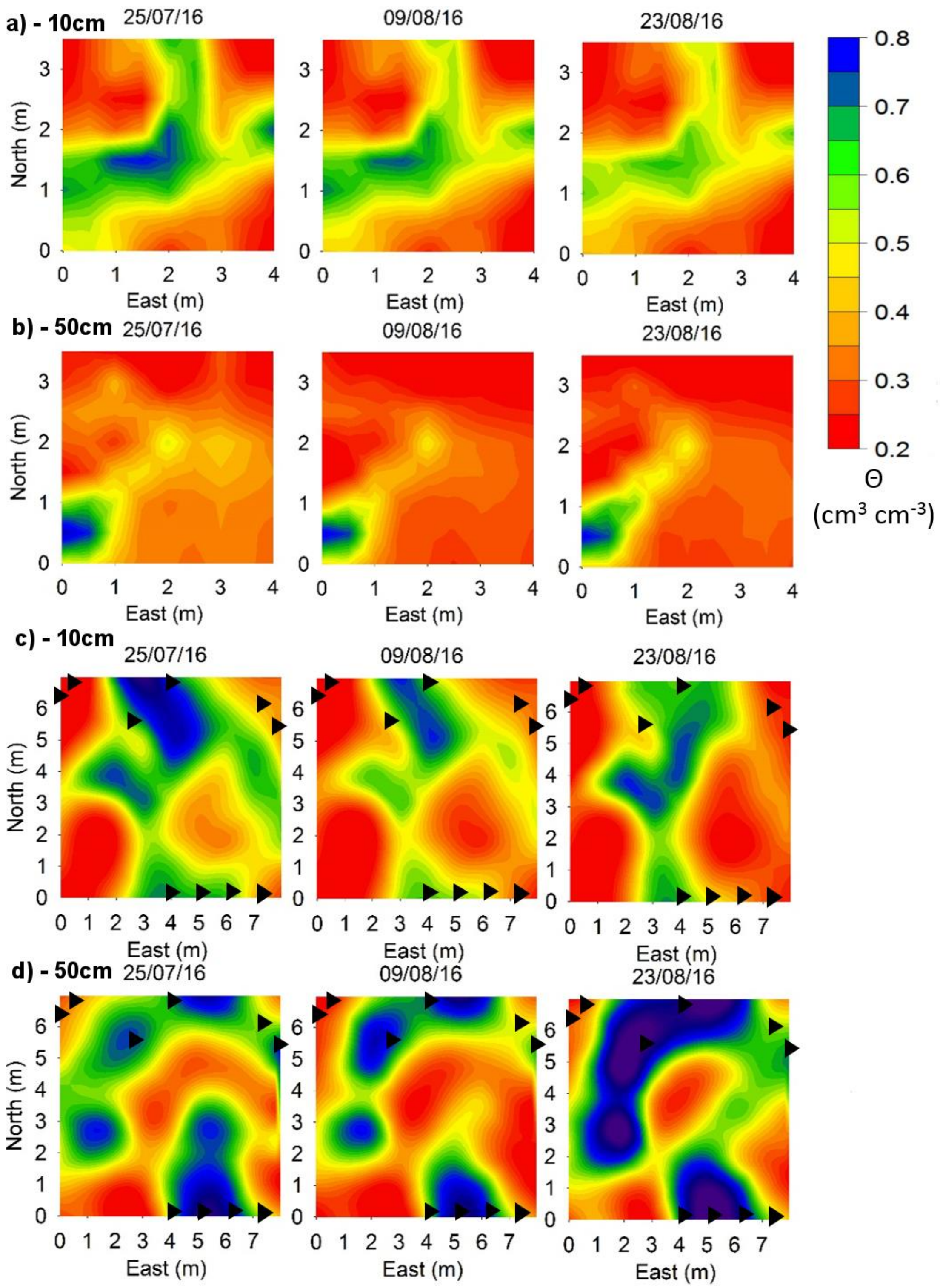

Fig. 7: Drying cycle from 25/07/16 to 23/08/16 at the heather sites 0.1 m (a) and 0.5 m (b) depths, and the forest sites 0.1 m (c) and 0.5 m (d) depths. Black triangles are tree locations.

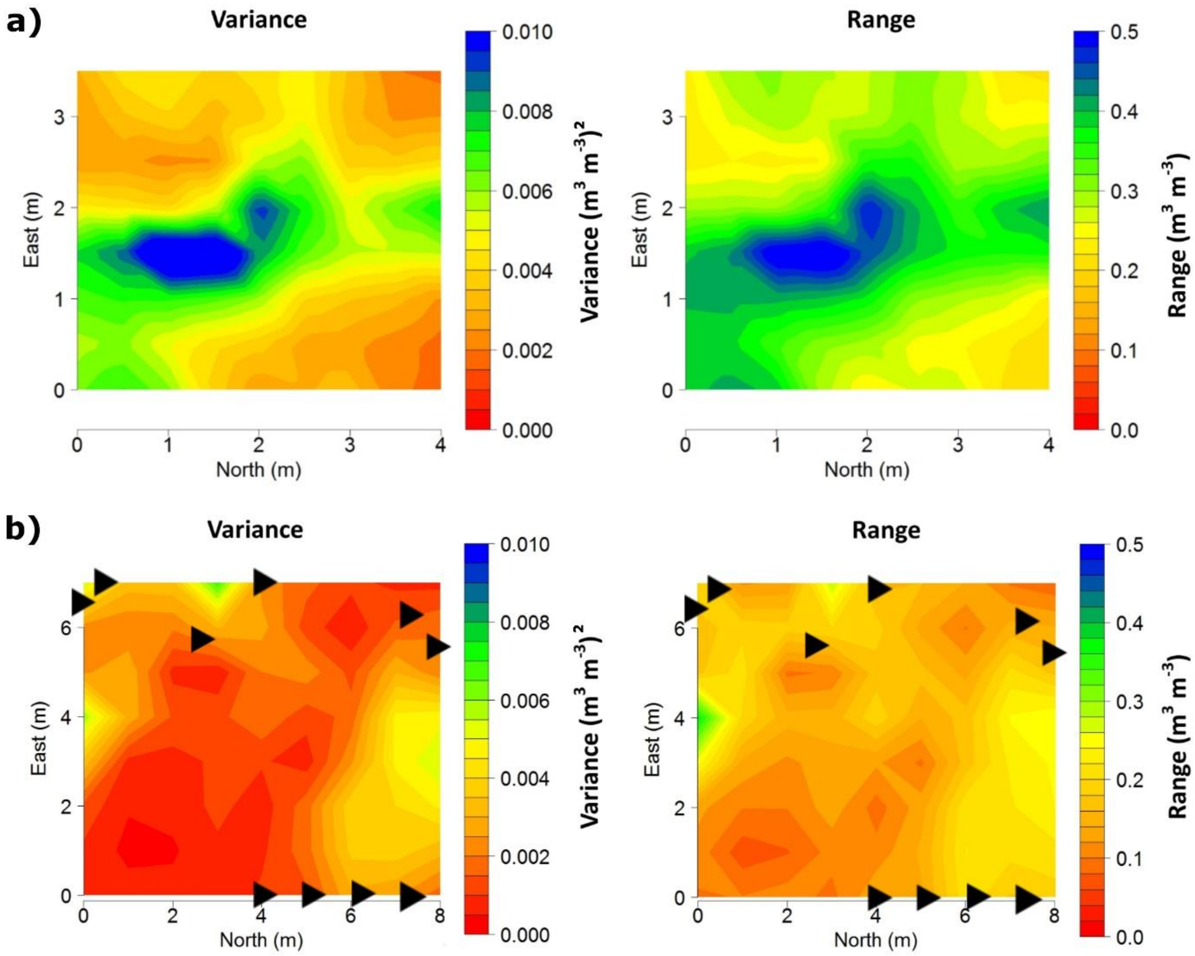

Fig. 8: Plots for temporal variance and range of VSM at 0.1 m depth for a) heather and b) forest sites.

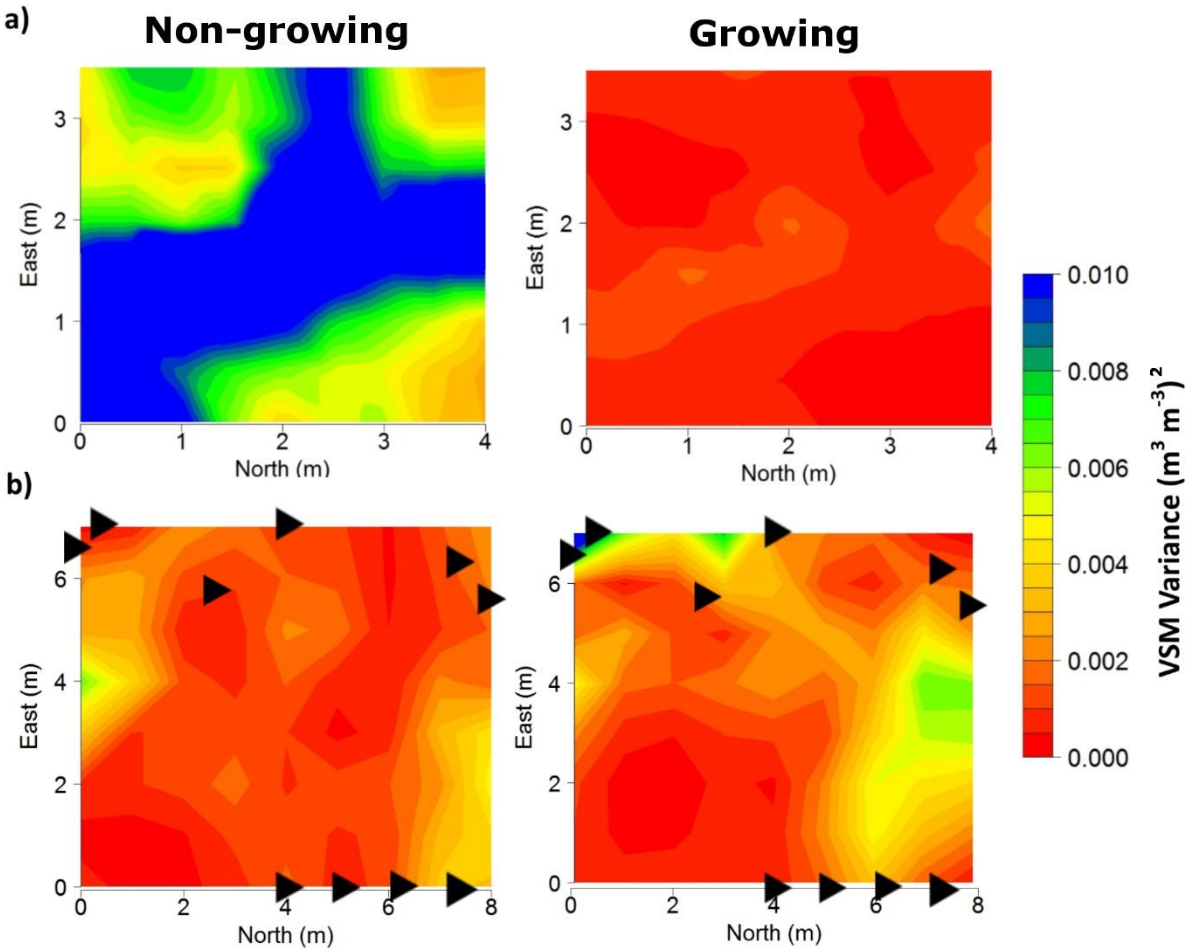

Fig. 9: VSM temporal variance plots for 0.1 m depth for the growing and non-growing season for a) the heather site and b) the forest site.

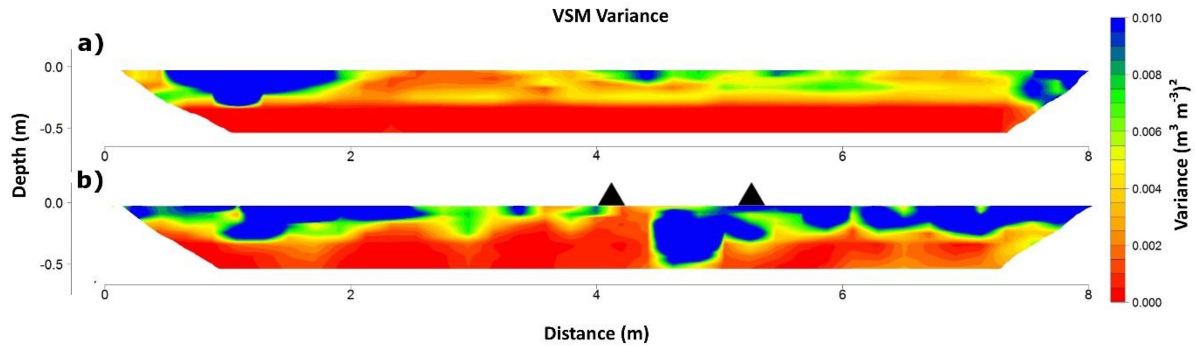

Fig. 10: Transects showing, a) the VSM statistical temporal variance between surveys for the heather site, and, b) the VSM statistical temporal variance between surveys for the forest site, Black triangles show position of scots pine.

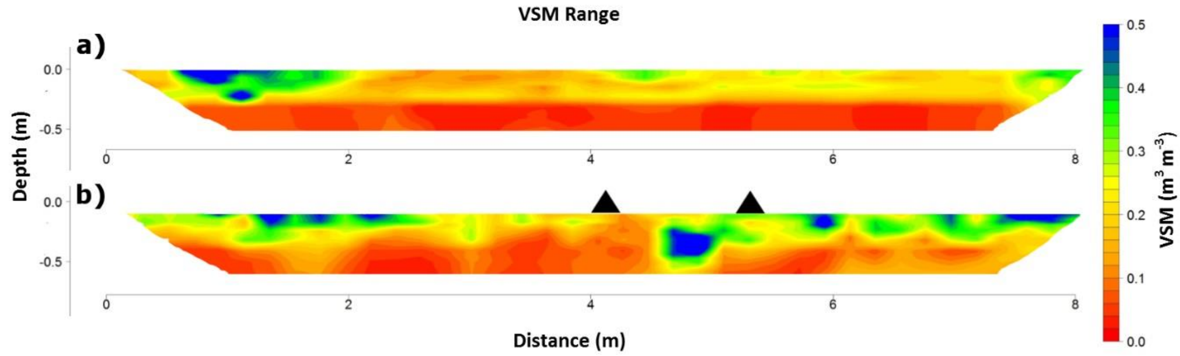

Fig. 11: Transects showing, a) the range of VSM temporal change between surveys for the heather site, and, b) range of VSM temporal change between surveys for the forest site. Black triangles show position of scots pine.